2006-01-01

All-Fiber Multimode-Interference-Based-Refractometer Sensor:Proposal and Design

Qian Wang
Dublin Institute of Technology

Gerald Farrell
Dublin Institute of Technology, gerald.farrell@dit.ie

Recommended Citation
Wang, Q., Farrell, G.:All-Fiber Multimode-Interference-Based-Refractometer Sensor:Proposal and Design. Optics Letters, Vol.31 (3), 2006, pp.317-319

All-fiber multimode-interference-based refractometer sensor: proposal and design

Qian Wang and Gerald Farrell

Applied Optoelectronics Centre, School of Electronics and Communications Engineering, Dublin Institute of Technology, Kevin Street, Dublin 8, Ireland

Received September 15, 2005; revised November 2, 2005; accepted November 4, 2005

A novel all-fiber refractometer sensor is proposed, which is based on multimode interference in the multimode fiber core section sandwiched between two single-mode fibers. A wide-angle beam propagation method in the cylindrical coordinate is employed as the modeling tool for simulation and design of the proposed refractometer sensor. The design for a refractometer is presented that shows that the refractometer would have an estimated resolution of 5.4×10^{-5} for refractive indices from 1.33 to 1.45 and of 3.3×10^{-5} for refractive indices from 1.38 to 1.45 through the choice of an appropriate length of the multimode fiber core section. © 2006 Optical Society of America

OCIS codes: 060.2370, 060.2340, 230.0230.

Optical refractometer sensors based on waveguide technology are promising and attractive in chemical and biotechnological applications for their superior advantages, such as high sensitivity, immunity to electromagnetic interference, and compact size. Several types of integrated optical waveguide or optical-fiber-based refractometer have been proposed in recent publications. Examples of integrated optical waveguide-based refractometers include bend-loss waveguides, planar antiresonant reflecting optical waveguides, and integrated Mach–Zehnder interferometers.[1–3] Refractometers based on fiber gap or fiber-to-planar polymer-waveguide couplers have also been presented in Refs. 4–6, respectively. As an alternative to these existing refractometers, a novel all-fiber refractometer sensor based on multimode interference in the multimode fiber core section is proposed and designed in this Letter.

The proposed refractometer sensor consists of input and output single-mode fibers (SMFs) and a sandwiched section of multimode fiber (MMF) core with a specific length (see Fig. 1). For the refractive index measurement the section of multimode fiber core is surrounded by the liquid sample, and with suitable calibration the refractive index of the liquid sample can be determined by measuring the light intensity from the output SMF. This single-mode–multimode–single-mode structure has been used as a microbend sensor and refractometer in Refs. 7 and 8. In Ref. 8 the MMF worked as a cavity element, and the refractive index of the surrounding liquid was determined by detecting the wavelength shift of the Fabry–Perot resonator.

The operating mechanism of the refractometer in this paper is based on the multimode interference (MMI) and corresponding self-image phenomena occurring in the multimode fiber section, for which the surrounded liquid sample works as the cladding medium. Multimode interference in the planar waveguide has been intensively investigated, and the self-image phenomena is well known and widely employed in developing optical couplers and combiners.[9] Compared with the planar waveguide case, there are few investigations of MMI in a multimode fiber section other than in Ref. 10, where MMI was employed in a displacement sensor by placing a mirror at the end of the MMF and in Ref. 11, where it was used in a fiber lens.

Within the proposed configuration, when the light field propagating along the input SMF enters the MMF section, similarly to the planar-waveguide-based MMI coupler, high-order eigenmodes of the MMF are excited and interference between different modes occurs while the beam propagates along the MMF section. The light is coupled into the output SMF at the end of the MMF section. With an optimal design, different refractive indices of the surrounding liquid sample can correspond to different transmission losses of the refractometer.

In order to let us carry out the optimal design of the refractometer, a wide-angle beam propagation method (BPM) in a cylindrical coordinate system is employed to simulate light propagation within the MMF section. Take the slowly varying envelope approximation, i.e., $E(r,z)=\hat{E}(r,z)\exp(jkn_0z)$ (where n_0 is the reference refractive index). For $\hat{E}(r,z)$, the corresponding beam propagation equation is

$$\frac{\partial\hat{E}}{\partial z}=\left[\left(\frac{j}{2kn_0}P\right)\Big/\left(1-\frac{j}{2kn_0}\frac{\partial}{\partial z}\right)\right]\hat{E}, \qquad (1)$$

where $P\hat{E}=[(\partial^2\hat{E}/\partial r^2)+(1/r)(\partial\hat{E}/\partial r)+k^2[n^2(r,z)-n_0^2]\hat{E}]$. With the Padé approximation, Eq. (1) has the form of $\partial\hat{E}/\partial z=(jN/D)\hat{E}$, where N and D are polynomials of operator P. Applying the Crank–Nicholson

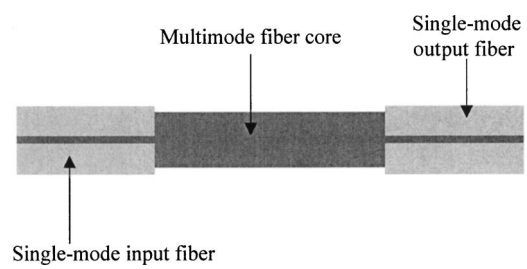

Fig. 1. Configuration of the proposed refractometer.

0146-9592/06/030317-3/$15.00

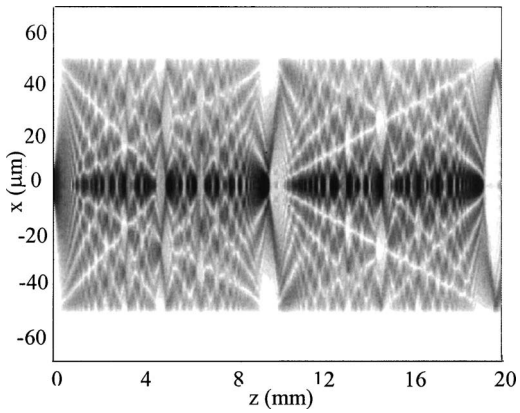

Fig. 2. Amplitude distribution of the propagation field within the multimode fiber section.

finite-difference scheme, $\hat{E}^{n+1}=[(D+j(\Delta z/2)N)/(D-j(\Delta z/2)N)]\hat{E}^{n}$. Factored in terms of m roots, i.e., $\hat{E}^{n+1}=[\Pi_{i=1}^{m}(1+a_iP)/\Pi_{i=1}^{m}(1+a_i^*P)]\hat{E}^{n}$, Eq. (1) can be solved iteratively.[12] For the ith step, we have

$$a_i^*\eta_-\hat{E}_{p-1}^{n+i/m}+[1+a_i^*\zeta]\hat{E}_p^{n+i/m}+a_i^*\eta_+\hat{E}_{p+1}^{n+i/m}$$
$$=a_i\eta_-\hat{E}_{p-1}^{n+i-1/m}+[1+a_i\zeta]\hat{E}_{p-1}^{n+i-1/m}+a_i\eta_+\hat{E}_{p+1}^{n+i-1/m}, \quad (2)$$

where $\eta_\pm=1/\Delta r^2\pm 1/2r\Delta r$ and $\zeta=k^2(n^2-n_0^2)-2/\Delta r^2$; a_i and $a_i^*(i=1,2\ldots,n)$ are determined by the N and D polynomials. At the fiber axis, Eq. (2) contains parameter r in the denominator of its coefficient. Therefore, as $r\to 0$ at the fiber axis, L' Hôpital's rule is used as before in Ref. 13, and the corresponding equation becomes

$$\left\{1+a_i^*\left[k^2(n^2-n_0^2)-\frac{4}{\Delta r^2}\right]\right\}\hat{E}_0^{n+i/m}+a_i^*\frac{4}{\Delta r^2}\hat{E}_1^{n+i/m}$$
$$=\left\{1+a_i\left[k^2(n^2-n_0^2)-\frac{4}{\Delta r^2}\right]\right\}\hat{E}_0^{n+(i-1)/m}$$
$$+a_i\left[\frac{4}{\Delta r^2}\right]\hat{E}_1^{n(i-1)/m}. \quad (3)$$

In practical calculations, based on the circular symmetric characteristic of the proposed structure, only the half-plane of the proposed structure, i.e., $0\leqslant r\leqslant R$, is used as the calculation area, and the perfectly matched layer is employed at the boundary of the calculation area[14] ($r=R$).

As a numerical example, light propagation in the multimode fiber section is simulated. An eigenmode for the standard single-mode fiber (SMF28) at a wavelength of 1550 nm is used as the input field. For the multimode fiber section, the refractive index of the core is $n_r=1.47$, and the core radius is $r_{co}=50\ \mu$m. The refractive index of the surrounding liquid sample is chosen to be $n=1.40$. For the above wide-angle BPM, the corresponding amplitude distribution of the propagation field is presented in Fig. 2.

For a given multimode fiber, i.e., given the refractive index profile, the length of the sandwiched multimode fiber section is crucial for building a one-to-one relationship between the refractive index of the liquid sample and the transmission loss of the device within the desired measurable refractive index range. To determine the optimal length of the multimode fiber section, a straightforward method is to scan the parameter space, which consists of the length of the multimode fiber section and the refractive index of the surrounding liquid sample with the presented BPM. To save computational time, the overlap integral method is used to calculate the transmission loss (decibels) as approximately

$$L_s(l)=10\log_{10}\left[\frac{\left|\int_0^\infty E(l,r)F(r)r\mathrm{d}r\right|^2}{\int_0^\infty|E(l,r)|^2r\mathrm{d}r\int_0^\infty|F(r)|^2r\mathrm{d}r}\right], \quad (4)$$

where l is the length of the multimode fiber section, $E(l,r)$ is the calculated field at the interface between the multimode fiber section, and the single-mode output fiber, and $F(r)$ is the eigenmode of the single-mode output fiber.

As a design example, the fiber parameters chosen are the same as those in the above numerical example. Since the multimode interference effect in the MMF section is utilized and the surrounding liquid works as the cladding layer, the measurable refractive index of the surrounding liquid is supposed to be less than the refractive index of the MMF core section. In this design example, given the core refractive index of 1.47, a desirable measurement range for the refractive index is from 1.33 to 1.45 (the typical refractive indices of many liquids are no less than 1.33). Simulation results presented in Fig. 2 show that the light converges periodically while propagating in the multimode fiber section. The first convergence occurs within the length range from 9 to 10 mm. Therefore transmission losses for the desirable refractive index range, i.e., from 1.33 to 1.45, are scanned around this length. The corresponding result is presented in Fig. 3.

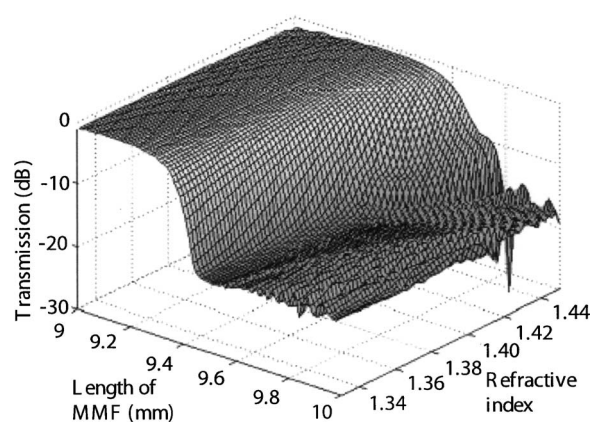

Fig. 3. Transmission losses versus length of MMF and refractive index.

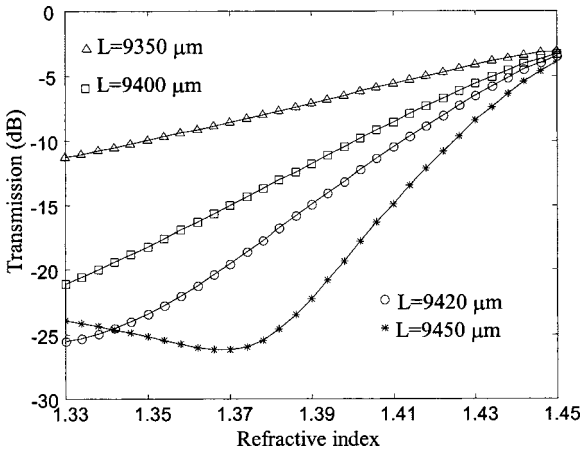

Fig. 4. One-to-one relationships between the transmission losses and refractive index at designed MMF lengths.

By inspection from Fig. 3 it is clear that the optimal length should lie in the vicinity of 9400 μm for the required refractive index range. Therefore, transmission losses versus refractive index for four lengths, $L=9350$, 9400, 9420, 9450 μm, are plotted in Fig. 4, which are based on simulations of light propagating through the whole structure. Eigenmodes of the MMF section are determined by the surrounding refractive index, and the multimode interference in MMF is affected correspondingly. Therefore, the converging position of the light varies for different surrounding refractive indices, and the transmission of the structure varies consequently.

Figure 4 shows one-to-one relationships between the transmission losses and the refractive index when the length is no bigger than 9420 μm. The transmission loss curve for a length of MMF $l=9420$ μm shows a discrimination range from −25.56 to −3.47 dB almost linearly over the whole refractive index range. It is known that the typical precision of a commercial optical powermeter is about 0.01 dB. Therefore the designed refractometer sensor for $l=9420$ μm has an estimated resolution of 5.4×10^{-5}. If the desirable measurement range is from 1.38 to 1.45, an estimated resolution of 3.3×10^{-5} is achieved when the length of the MMF is $l=9450$ μm. These results are competitive as compared with existing types as presented in Refs. 1 and 2.

Numerical simulation indicates that this multimode-interference-based refractometer sensor is wavelength sensitive. To achieve its maximal sensitivity for the refractive index of the surrounding liquid, the specific optimal length of the MMF section depends on the wavelength in use. For example, for the wavelength of 1550 nm, the optimal length is 9420 mm, whereas for 1600 nm, it is 9120 mm.

In this Letter, we have proposed a novel all-fiber refractometer sensor for a liquid sample that contains a multimode fiber core section sandwiched between two single-mode fibers and utilizes the multimode interference in the multimode core section. The wide-angle beam propagation method in the cylindrical coordinate has been employed for numerical simulation and design. The designed refractometer shows an estimated resolution of 5.4×10^{-5} for refractive index range from 1.33 to 1.45, and 3.3×10^{-5} for the refractive index from 1.38 to 1.45, while offering a much simpler configuration as compared with existing waveguide-based optical refractometer sensors. Corresponding experimental work for this refractometer sensor is ongoing.

Q. Wang's e-mail address is Qian.wang@dit.ie.

References

1. G. J. Veldhuis, L. E. W. van der Veen, and P. V. Lambeck, J. Lightwave Technol. **17**, 857 (1999).
2. R. Bernini, S. Campopiano, C. de Boer, P. M. Sarro, and L. Zeni, IEEE Sens. J. **3**, 652 (2003).
3. B. Maisenholder, H. P. Zappe, M. Moser, P. Riel, R. E. Kunz, and J. Edlinger, Electron. Lett. **35**, 986 (1997).
4. Z. Zhou and F. F. Liu, J. Opt. Soc. Am. A **8**, 322 (1991).
5. W. Johnstone, G. Thursby, D. Moodie, and K. McCallion, Opt. Lett. **17**, 1538 (1992).
6. G. Raizada and B. P. Pal, Opt. Lett. **21**, 399 (1996).
7. A. Kumar, R. K. Varshney, A. C. Siny, and P. Sharma, Opt. Commun. **219**, 215 (2003).
8. Y. Jung, Y. S. Jeong, J. Kim, S. Yoo, and K. Oh, in *ECOC 2004 Proceedings*, 3, paper We4.P.031.
9. L. B. Soldano and E. C. M. Pennings, J. Lightwave Technol. **13**, 615 (1995).
10. A. Mehta, W. S. Mohammed, and E. G. Johnson, IEEE Photon. Technol. Lett. **15**, 1129 (2003).
11. W. S. Mohammed, A. Mehta, and E. G. Johnson, J. Lightwave Technol. **22**, 469 (2004).
12. G. R. Hadley, Opt. Lett. **17**, 1743 (1992).
13. J. Yamauchi, Y. Akimoto, M. Nibe, and H. Nakano, IEEE Photon. Technol. Lett. **8**, 236 (1996).
14. W. P. Huang, C. L. Xu, W. Lui, and K. Yokoyama, IEEE Photon. Technol. Lett. **8**, 649 (1996).